13th World Conference on Earthquake Engineering
Vancouver, B.C., Canada
August 1-6, 2004
Paper No. 2988

PHYSICAL DUCTILITY DEMAND SPECTRA FOR EARTHQUAKE GROUND MOTIONS CONTAINING SEVERE PULSES

Otton LARA[1] , Renato PARODI[2], José CENTENO[3] and Vitelmo V. BERTERO[4]

SUMMARY

Earthquake (EQ) Structural analysis and design require a reliable estimation of the demands, in particular for the appropriate application of Performance Based Seismic Design (PBSD). For a given EQ the ground motions recorded on rock are different from those obtained in soft soil, even for the same epicentral distance. EQ Ground Motions (EQGMs) recorded close and normal to the fault differ from those recorded close but parallel to the fault and both are different from those recorded far from the fault. It is known that EQGMs recorded close to the fault show severe pulses that have been the cause of severe Structural damage. This fact is considered only partially by current codes which recommend the use of near fault factors that affect only the required base shear. For Inelastic design those codes recommend to reduce the elastic spectral amplitude by reduction factors that are constant for all the periods. The validity of this procedure has been questioned and shown to be inadequate. The objectives of this investigation were to determine a procedure to identify severe pulses in EQGMs recorded close or far from the fault. Then, to study the effects of those pulses on the elastic and inelastic response of Single Degree of Freedom (SDOF) structures. Later, it was demonstrated that the cyclic ductility ratio allows to obtain a reliable inelastic demand spectra. Finally, Physical Ductility Spectra (PDS) are presented for EQGM records obtained close and far from the fault. It is demonstrated that PDS offer a more reliable estimation of inelastic displacement demands.

INTRODUCTION

Even though the study of the effects of severe pulses contained in Earthquake Ground Motion Records (EQGMRs) has not been investigated by too many researches, the works by Sasani, Bertero and Anderson [1], Sasani [2] and Alavi and Krawinkler [3], have focused on the use of simple pulses to replace the original record. The results indicate:

1. The representation of EQGMRs containing severe pulses, using simple pulses is an approximation since the problem is very complex. The approximation becomes less reliable when the ground velocity contains a train of pulses.
2. The parameters that define a severe pulse: Intensity, type and duration can be identified by simple pulses that simulate EQGMRs that show a single peak in the EVDS.

[1] Professor Instituto de Investigaciones y Estudios Avanzados (IIEA), Universidad de Guayaquil, Ecuador.
Escuela Superior Politécnica del Litoral (ESPOL), Guayaquil - Ecuador
e-mail: sismica@gye.satnet.net
[2] Graduate student, IIEA
[3] Civil engineer graduating student, ESPOL
[4] Professor Emeritus University of California, Berkeley. Pacific Earthquake Engineering Research Center. Richmond, Ca.

3. The use of simple pulses has helped to a better understanding of the linear and non-linear response of structures subjected to such pulses.

Severe acceleration pulse can be defined, from the point of view of the ground record, as a large amplitude acceleration value associated to a long duration. In some EQGMRs there is a very well defined severe pulse, whereas in some others there are two severe pulses and in others there is a train of severe pulses. The effect of any acceleration pulse, measured between the zero crossings of the amplitude, can be visualized in the ground velocity. Bertero [4] showed that within the duration of an acceleration pulse it is possible to measure the ground velocity from one peak to the other.

In the case of more than one severe pulse, one of them will be the most severe and the one that will induce the largest measured peak to peak ground velocity.

The question is what is a severe pulse from the point of view of the structure. All acceleration records contain pulses which are severe for some structures and are insignificant for others, therefore it is important to study, first, through the frequency domain, what are the important frequencies of the ground motion affecting the shape of Elastic and Inelastic Demand Spectra (EDS and IDS) and then through non linear time history analysis, how the structures are affected by the ground motions.

The behavior of structures subjected to EQGMRs containing pulses vary depending on if the record contains one or more pulses or if the structure has been designed to enter the nonlinear range or not and on the frequency content of the record. Of course the response will depend, besides, on the period and on the damping of the structural system.

In the present investigation Single Degree of Freedom (SDOF) structures with 5% damping will be studied. The first objective of this research deals with a procedure to identify the presence of pulses out of a ground motion and to determine how important is not only the most severe pulse but the motion before and after in the definition of the EDS and IDS. The second objective refers to the study of what are the critical ground motions, containing pulses, for the non linear time-history response of SDOF structures.

ELASTIC PROCEDURES TO UNDERSTAND EQGMR's CONTAINING SEVERE PULSES

In order to understand how the severe pulse and in some records, the several severe pulses, as well as the rest of the ground record affect the shape of the Elastic Demand Spectra (EDS) and that of the Inelastic Demand Spectra (IDS), a study of several EQGMRs is performed.

Table 1 shows a list of EQGMRs provided by Krawinkler [5]. In this list there are 22 ground motion records obtained close to the fault. Krawinkler [5], classified the records such that 15 of them show forward directivity effects, and 7 backward directivity. The lists shows besides, 40 records, obtained at places more than 10 Km away from the fault, that were called ordinary records by Krawinkler [5], because, apparently, they do not contain severe pulses.

TABLE 1. CHARACTERISTICS OF GROUND MOTIONS

NEAR FAULT GROUND MOTION								
Designation	Earthquake	Station	Directivity	M_w	R(km)	PGA (cm/s^2)	MVGV (cm/s)	t_d (s)
CM92petr	Mendocino, 1992	Petrolia	backward	7,1	8,5	625,60	205,67	0,56
IV79bond	Imperial Valley, 1979	Bond's Corn	backward	6,5	2,4	770,50	83,6	0,35
LP89corr	Loma Prieta, 1989	Corralitos	backward	7,0	3,4	448,62	96,09	0,43
MH84hall	Morgan Hill, 1984	Halls Valley	backward	6,2	2,4	300,00	64,71	0,36
NR94nord	Northridge, 1994	Arleta	backward	6,7	9,2	232,00	30,21	0,28
TB78tab	Tabas, 1978	Tabas	backward	7,4	1,2	882,85	202,4	0,76
					Average =	543,26	113,78	0,46
					σ =	260,29	73,37	0,18
Designation	Earthquake	Station	Directivity	M_w	R(km)	PGA (cm/s^2)	MVGV (cm/s)	t_d (s)
EZ92erzi	Erzincan, 1992	Erzincan	forward	6,7	2,0	423,90	153,93	0,57
IV79ar06	Imperial Valley, 1979	Array 6	forward	6,5	1,2	424,00	194,46	1,37
IV79melo	Imperial Valley, 1979	Meloland	forward	6,5	0,0	371,91	167,80	1,26
KB95kobj	Kobe, 1995	JMA	forward	6,9	0,6	1067,20	295,53	0,42
KB95kpi1	Kobe, 1995	Port Island	forward	6,9	3,7	425,73	180,79	0,83
KB95tato	Kobe, 1995	Takatori	forward	6,9	1,5	771,10	296,02	0,66
LP89lex	Loma Prieta, 1989	Lexington	forward	7,0	6,3	672,86	243,39	0,60
LP89lgpc	Loma Prieta, 1989	Los Gatos	forward	7,0	3,5	703,78	268,39	1,13
MH84andd	Morgan Hill, 1984	Anderson D	forward	6,2	4,5	274,00	49,80	0,31
MH84cyld	Morgan Hill, 1984	Coyote L D	forward	6,2	0,1	711,00	125,70	0,35
NR94newh	Northridge, 1994	Newhall	forward	6,7	7,1	709,25	177,70	0,34
NR94rrs	Northridge, 1994	Rinaldi	forward	6,7	7,5	872,70	254,60	0,44
NR94spva	Northridge, 1994	Sepulveda	forward	6,7	8,9	714,61	75,21	0,26
NR94sylm	Northridge, 1994	Olive View	forward	6,7	6,4	718,00	140,17	0,66
					Average =	632,86	187,39	0,66
					σ =	219,24	76,94	0,36

ORDINARY RECORDS								
Designation	Earthquake	Station	Directivity	M_w	R(km)	PGA (cm/s^2)	MVGV (cm/s)	t_d (s)
IV79cal	Imperial Valley,1979	Calipatria Fire Station		6,5	23,8	76,91	14,63	1,37
IV79chi	Imperial Valley,1979	Chihuahua		6,5	28,7	264,87	34,82	0,32
IV79cmp	Imperial Valley,1979	Compuertas		6,5	32,6	182,47	20,10	0,22
IV79e01	Imperial Valley,1979	El Centro Array		6,5	15,5	136,36	19,96	0,52
IV79e12	Imperial Valley,1979	El Centro Array		6,5	18,2	113,80	29,32	1,41
IV79e13	Imperial Valley,1979	El Centro Array		6,5	18,2	136,36	16,92	0,69
IV79nil	Imperial Valley,1979	Niland Fire Station		6,5	35,9	106,93	15,36	0,28
IV79pls	Imperial Valley,1979	Plaster City		6,5	31,7	55,72	6,23	0,26
IV79qkp	Imperial Valley,1979	Cucapah		6,5	23,6	303,13	52,88	0,73
IV79wsm	Imperial Valley,1979	Westmorland Fire Station		6,5	15,1	107,91	24,16	0,96
LP89agw	Loma Prieta, 1989	Agnews State Hospital		7,0	28,2	168,00	17,50	0,34
LP89cap	Loma Prieta, 1989	Capitola		7,0	14,5	443,00	57,00	0,28
LP89g03	Loma Prieta, 1989	Gilroy Array #3		7,0	14,4	360,00	45,00	0,35
LP89g04	Loma Prieta, 1989	Gilroy Array #4		7,0	16,1	207,90	59,34	0,77
LP89gmr	Loma Prieta, 1989	Gilroy Array #7		7,0	24,2	221,00	23,00	0,27
LP89hch	Loma Prieta, 1989	Hollister City Hall		7,0	28,2	242,00	58,50	0,35
LP89hda	Loma Prieta, 1989	Hollister Differential Array		7,0	25,8	273,00	58,50	0,31
LP89hvr	Loma Prieta, 1989	Halls Valley		6,9	31,6	131,55	22,18	0,44
LP89sjw	Loma Prieta, 1989	Salinas - John & Work		6,9	32,6	109,87	19,26	0,87
LP89slc	Loma Prieta, 1989	Palo Alto - SLAC Lab.		6,9	36,3	190,61	61,87	0,77
LP89svl	Loma Prieta, 1989	Sunnyvale-Colton Ave.		6,9	28,8	203,00	69,83	1,56
NR94cen	Northridge, 1994	LA - Centinela St.		6,7	30,9	315,49	38,31	0,56
NR94cnp	Northridge, 1994	Canoga Park - Topanga Can.		6,7	15,8	412,00	43,24	0,33
NR94far	Northridge, 1994	LA-N Fairing Rd		6,7	23,9	267,81	29,99	0,2
NR94fle	Northridge, 1994	LA-Fletcher Dr		6,7	29,5	235,40	40,92	0,36
NR94glp	Northridge, 1994	Glendale - Las Palmas		6,7	25,4	202,00	13,50	0,13
NR94hol	Northridge, 1994	LA - Hollywood Stor FF		6,7	25,5	226,00	27,37	0,59
NR94lh1	Northridge, 1994	Lake Hughes #1		6,7	36,3	84,96	16,54	0,42
NR94lv2	Northridge, 1994	Leona Valley #2		6,7	37,7	62,10	10,30	1,10
NR94lv6	Northridge, 1994	Leona Valley #6		6,7	38,5	174,00	21,69	0,34
NR94nya	Northridge, 1994	La Cresenta - New York		6,7	22,3	155,98	21,25	0,33
NR94pic	Northridge, 1994	LA - Pico & Sentous		6,7	32,7	182,466	18,90	0,23
NR94stc	Northridge, 1994	Northridge - 17645 Saticoy St.		6,7	13,3	361,01	53,52	0,44
NR94stn	Northridge, 1994	LA - Saturn St		6,7	30	465,00	59,17	0,29
NR94ver	Northridge, 1994	LA - E Vernon Ave.		6,7	39,3	150,93	16,96	0,64
SF71pel	San Fernando, 1971	LA - Hollywood Stor Lot		6,6	21,2	170,69	16,83	0,68
SH87bra	Superstition Hills, 1987	Brawley		6,7	18,2	153,04	18,42	0,31
SH87icc	Superstition Hills, 1987	El Centro Imp Co. Cent		6,7	13,9	351,20	28,40	0,22
SH87pls	Superstition Hills, 1987	Plaster City		6,7	21	182,00	38,56	0,43
SH87wsm	Superstition Hills, 1987	Westmorland Fire Station		6,7	13,3	168,73	29,61	1,4
					Average =	208,88	31,75	0,55
					σ =	102,85	17,33	0,37
M_w:	Moment Magnitude		MVGV:	Maximum Variation of the Ground Velocity				
R:	Distance from the site to the fault		td:	duration of the MVGV				
PGA:	Peak Ground Acceleration							

General observations of EQGMRs. Figure 1 shows the NR94stc record of the Northridge 1994 earthquake which is one of the ordinary records. Its maximum acceleration reaches 361 cm/sec^2 at about 4.7 secs and its duration is insignificant. The corresponding variation of the ground velocity reaches 25 cm/sec. Observing the ground velocity (Fig 1), the largest peak to peak value is 53.5 cm/sec located at about 8.86 secs. This largest value is the MVGV of the record and it is not associated to the maximum acceleration but it is indicating that at 8.86 secs there is a pulse in the acceleration record. The acceleration corresponding to the MVGV is about 200 cm/sec^2 and its duration is about 0.44 secs. Notice that the ground displacements are small, in the order of 10 cm.

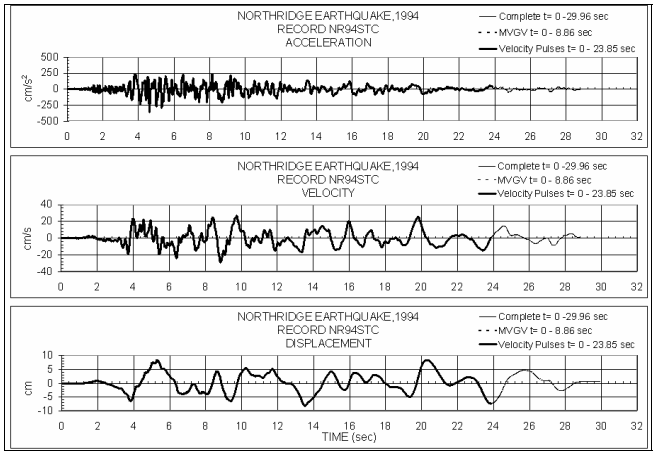

FIGURE 1. Record NR94stc

Consider now the EZ92erzi record of the Erzincan 1992 earthquake (Fig 2) which shows a forward directivity effect. The acceleration record shows several pulses, one of them with a maximum amplitude of 424 cm/sec^2 approximately, and a duration, td, of about 0.57 sec. The MVGV corresponding to this pulse, is 154 cm/sec (Fig 2). In this case the MVGV corresponds to the maximum acceleration of the record and induces a large ground displacement in the order of 43 cm.

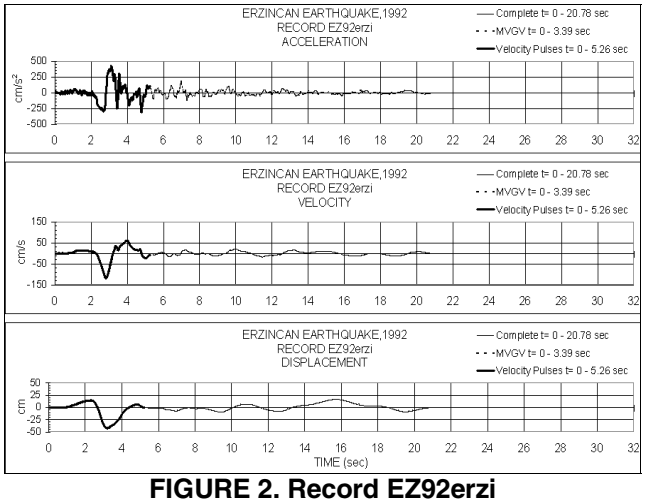

FIGURE 2. Record EZ92erzi

Comparing the MVGV associated to the largest pulse in both records, the difference is considerable as it is in all cases when comparing ordinary records with NFGMR. The MVGV of the latest are always related to a severe pulse (large acceleration with long duration), from the point of view of the record, while in ordinary records the MVGV is, in general, related to smaller accelerations with relatively long duration. How severe is a pulse for different SDOF structures will be analyzed under the non linear behavior of such SDOF structures.

Table 1 shows the MVGV calculated for the forward and backward directivity effect records, and for the ordinary records. Table 2 also shows the Moment Magnitude, (Mw), the distance from the fault to the site, the Peak Ground Acceleration (PGA) of the record, and the duration of the severe pulse related to the MVGV. Clearly, the MVGV of the forward directivity records (FDR) are larger than those of the backward directivity records (BDR) and are quite larger than the MVGV of the ordinary records.

Notice that the average of the MVGV of the FDR minus one standard deviation, 103.94 cm/sec, is almost equal to the average of MVGV of the BDR, 106.81 cm/sec, and 2.8 times the average of the MVGV of the ordinary records (36.15 cm/sec).

The average duration of the MVGV for the FDR is 1.3 times the duration of the MVGV of the BDR and 1.4 times that of the ordinary records.

It should be mentioned that the dispersion is very large, so the statistics shows only a tendency.

The above analysis of the records allows to begin to establish the differences between ordinary and FDR and BDR.

In what follows, in order to cover the first objective of this investigation, which is to try to find a way to identify the presence of pulses out of a ground motion, through the Fourier Spectra, the Elastic Velocity Demand Spectra (EVDS) and the Power of the acceleration record, a fraction of the record, capable of simulating a high percentage of the frequency content of the record and reproduce most of the Elastic Demand Spectra (EDS) as well as the Inelastic Demand Spectra (IDS) of the complete record is determined. It will be demonstrated that the Power is a way to define the duration of that fraction. Then, non linear analysis are carried out, using such fraction, in order to identify how SDOF structures are affected by ordinary or pulse type records.

Frequency content and Power of the records. In order to understand how the severe pulse or pulses contained in EQGMRs, as well as the motion before and after the main pulse, affects the Elastic and Inelastic Demand Spectra (EDS and IDS), a procedure by which the acceleration record is cut between t=0 and an appropriate time larger than zero is performed. The cuts are chosen according to the

ground velocity pulses and the Power of the record. Every piece of the record is then analyzed to obtain the Fourier transform. Later, EDS and IDS are obtained for every piece of the record and superimposed on the EDS and IDS of the complete and original record. In this way it will become clear what periods of the spectra are affected by the modified record.

The modifications are based on the ground velocity in the following way:

- The first cut corresponds to a piece of record that goes from t=0 to the end of the MVGV. If there are smaller pulses before the severe one, the modified record has taken them already into account.
- The second cut covers from t = 0 to the end of all the important velocity pulses that can follow after the MVGV. In this way if there are important pulses after the severe one, all of them will be taken into account.
- The velocity pulses considered in the second cut, coincide with the time when about 94% or more of the total Power has been reached.

Instead of drawing the Fourier amplitudes with respect to the frequency, the abscissa has been changed, so the period of the amplitudes is shown. Figure 3 shows the period content (thinner line) for some of the complete FDR, BDR and ordinary records of the list shown in table 1. This figure also shows the period content of the piece of record, first cut, that goes from t = 0 to the time when the MVGV is reached (dash line) as well as that of the piece, second cut, that goes from t = 0 to the time where all important ground velocity pulses have been taken into account (thicker line).

Clearly, the period content of the first piece does not resemble at all the period content of the complete record except for very short periods. This means that the piece of record that includes the MVGV can not represent the mid and long periods of the ground motion. Looking at the velocity ground motions there are several important pulses product of large accelerations and or large durations. If all of them are considered for the second cut, the period content of this piece of record is very similar to that of the complete record. This means that the motion that occurs after the MVGV must be taken into account.

The number of ground velocity pulses that must be considered to recreate almost all the frequency content of the records, coincides, in the FDR and BDR, with the 94%, on average, of the total Power that every record can reach. The time required to reach the 94% of the total power defines the time at which the second cut must be done. The Power content of a non periodic function is equal to the square of its continuous harmonics.

In ordinary records it is necessary to reach, on average, 97% of the total Power in order to find the time of the second cut.

Table 2 shows the time t_1, when the Power of the ground motion begins to rise from zero; time t_2, when the Power (Pt_2) reaches a high percentage of the total Power; the rise time of the Power: ($t_2 - t_1$); the value of the Power at the end of time t_2 (Pt_2); the Power at the end of the record (Pe) and the relation (Pt_2/Pe). The Power at the end of the record is the total Energy of the ground motion at the site.

TABLE 2. POWER OF GROUND MOTIONS

NEAR FAULT GROUND MOTION										
Designation	Earthquake	Station	Directivity	t_1 (s)	t_2 (s)	$t_2 - t_1$ (s)	$P\,t_2$ (cm^2/s^3)	D (s)	P e (cm^2/s^3)	$P\,t_2$ / Pe
CM92petr	Mendocino, 1992	Petrolia	backward	2,66	9,8	7,14	301005,64	80,0	339677,19	0,89
IV79bond	Imperial Valley, 1979	Bond's Corn	backward	2,72	13,21	10,49	354742,03	60,0	370314,28	0,96
LP89corr	Loma Prieta, 1989	Corralitos	backward	2,30	10,79	8,49	218392,10	60,0	225725,92	0,97
MH84hall	Morgan Hill, 1984	Halls Valley	backward	1,66	12,94	11,28	50191,16	60,0	52172,04	0,96
NR94nord	Northridge, 1994	Arleta	backward	3,14	16,42	13,28	57122,83	40,0	60574,02	0,94
TB78tab	Tabas, 1978	Tabas	backward	4,50	18,74	14,24	681961,48	50,0	768777,46	0,89
			Average =	2,83	13,65	10,82	2,77E+05		3,03E+05	93,40%
			σ =	0,96	3,38	2,72	2,34E+05		2,65E+05	3,76%

Designation	Earthquake	Station	Directivity	t_1 (s)	t_2 (s)	$t_2 - t_1$ (s)	P t2 (cm2/s3)	D (s)	P e (cm2/s3)	P t2 / Pe
EZ92erzi	Erzincan, 1992	Erzincan	forward	2,31	5,26	2,95	106231,19	20,8	125376,25	0,85
IV79ar06	Imperial Valley, 1979	Array 6	forward	2,46	10,05	7,59	99852,49	25,0	108624,02	0,92
IV79melo	Imperial Valley, 1979	Meloland	forward	3,69	9,50	5,81	82051,72	40,0	88804,42	0,92
KB95kobj	Kobe, 1995	JMA	forward	7,20	13,32	6,12	856000,54	20,8	911247,84	0,94
KB95kpi1	Kobe, 1995	Port Island	forward	13,32	22,20	8,88	147208,38	49,3	152333,24	0,97
KB95tato	Kobe, 1995	Takatori	forward	1,31	11,98	10,67	611370,16	60,0	648598,28	0,94
LP89lex	Loma Prieta, 1989	Lexington	forward	2,78	8,78	6,00	386711,72	40,1	389817,44	0,99
LP89lgpc	Loma Prieta, 1989	Los Gatos	forward	6,31	13,73	7,42	696329,53	39,1	749203,30	0,93
MH84andd	Morgan Hill, 1984	Anderson D	forward	2,20	9,94	7,74	48097,62	56,9	49861,20	0,96
MH84cyld	Morgan Hill, 1984	Coyote L D	forward	2,35	7,95	5,60	250505,22	200,0	254541,92	0,98
NR94newh	Northridge, 1994	Newhall	forward	3,70	9,52	5,82	380657,23	28,3	396902,82	0,96
NR94rrs	Northridge, 1994	Rinaldi	forward	2,10	6,89	4,79	475183,17	60,0	504364,93	0,94
NR94spva	Northridge, 1994	Sepulveda	forward	2,92	12,66	9,74	352943,48	60,0	367263,65	0,96
NR94sylm	Northridge, 1994	Olive View	forward	3,22	9,58	6,36	221541,43	47,8	232062,30	0,95
			Average =	3,99	10,81	6,82	3,37E+05		3,56E+05	94,47%
			σ =	3,14	4,06	2,03	2,50E+05		2,66E+05	3,52%

ORDINARY RECORDS

Designation	Earthquake	Station	Directivity	t_1 (s)	t_2 (s)	$t_2 - t_1$ (s)	P t2 (cm2/s3)	D (s)	P e (cm2/s3)	P t2 / Pe
IV79cal	Imperial Valley,1979	Calipatria Fire Station		7,09	27,39	20,30	5639,6357	39,5	6199,1524	0,91
IV79chi	Imperial Valley,1979	Chihuahua		3,94	34,76	30,82	71660,63	40,0	71922,89	1,00
IV79cmp	Imperial Valley,1979	Compuertas		5,29	30,02	24,73	23443,477	36,0	23956,2171	0,98
IV79e01	Imperial Valley,1979	El Centro Array		6,15	20,68	14,53	16051,82	39,0	16943,76	0,95
IV79e12	Imperial Valley,1979	El Centro Array		4,92	31,46	26,54	20183,20	39,0	20394,33	0,99
IV79e13	Imperial Valley,1979	El Centro Array		4,92	31,67	26,75	15728,50	39,5	16002,32	0,98
IV79nil	Imperial Valley,1979	Niland Fire Station		5,25	20,45	15,20	10044,57	40,0	11350,58	0,88
IV79pls	Imperial Valley,1979	Plaster City		2,46	17,62	15,17	3456,65	18,7	3466,12	1,00
IV79qkp	Imperial Valley,1979	Cucapah		4,71	22,08	17,38	60713,02	40,0	63632,4003	0,95
IV79wsm	Imperial Valley,1979	Westmorland Fire Station		4,46	27,75	23,29	6910,43	40,0	7395,3711	0,93
LP89agw	Loma Prieta, 1989	Agnews State Hospital		6,22	24,27	18,05	25847,65	24,3	25847,65	1,00
LP89cap	Loma Prieta, 1989	Capitola		2,50	17,27	14,77	140934,70	40,0	147541,80	0,96
LP89g03	Loma Prieta, 1989	Gilroy Array #3		2,60	8,81	6,21	71810,28	39,9	83775,58	0,86
LP89g04	Loma Prieta, 1989	Gilroy Array #4		3,90	39,96	36,06	59470,35	40,0	59470,35	1,00
LP89gmr	Loma Prieta, 1989	Gilroy Array #7		3,62	20,00	16,38	47939,78	40,0	48738,10	0,98
LP89hch	Loma Prieta, 1989	Hollister City Hall		4,25	24,30	20,05	48554,49	39,1	50913,04	0,95
LP89hda	Loma Prieta, 1989	Hollister Differential Array		4,32	24,83	20,51	62925,37	39,6	64634,89	0,97
LP89hvr	Loma Prieta, 1989	Halls Valley		3,87	18,11	14,24	14536,25	40,0	16105,43	0,90
LP89sjw	Loma Prieta, 1989	Salinas - John & Work		5,83	21,67	15,84	13600,52	40,0	14839,91	0,92
LP89slc	Loma Prieta, 1989	Palo Alto - SLAC Lab.		6,23	20,09	13,86	32446,68	39,6	34047,04	0,95
LP89svl	Loma Prieta, 1989	Sunnyvale-Colton Ave.		5,00	31,34	26,34	39944,75	39,3	40567,76	0,98
NR94cen	Northridge, 1994	LA - Centinela St.		5,00	24,15	19,15	60304,59	30,0	61144,53	0,99
NR94cnp	Northridge, 1994	Canoga Park - Topanga Can.		2,91	24,96	22,05	172686,03	25,0	172686,03	1,00
NR94far	Northridge, 1994	LA-N Fairing Rd		2,87	11,59	8,72	41104,81	30,0	41104,81	1,00
NR94fle	Northridge, 1994	LA-Fletcher Dr		4,39	29,96	25,57	40261,05	30,0	40261,05	1,00
NR94glp	Northridge, 1994	Glendale - Las Palmas		4,15	17,31	13,16	35313,18	30,0	36901,65	0,96
NR94hol	Northridge, 1994	LA - Hollywood Stor FF		4,14	20,2	16,06	53409,66	40,0	54981,20	0,97
NR94lh1	Northridge, 1994	Lake Hughes #1		2,00	19,46	17,46	9572,43	32,0	9940,24	0,96
NR94lv2	Northridge, 1994	Leona Valley #2		1,90	14,78	12,88	3345,84	32,0	3663,16	0,91
NR94lv6	Northridge, 1994	Leona Valley #6		4,22	19,88	15,66	19722,64	32,0	20231,61	0,97
NR94nya	Northridge, 1994	La Cresenta - New York		4,03	15,57	11,54	16923,32	30,0	17670,11	0,96
NR94pic	Northridge, 1994	LA - Pico & Sentous		7,25	28,84	21,59	15890,33	40,0	16223,35	0,98
NR94stc	Northridge, 1994	Northridge - 17645 Saticoy St.		3,67	23,85	20,18	119974,34	30,0	121621,92	0,99
NR94stn	Northridge, 1994	LA - Saturn St		4,84	31,56	26,72	68975,47	31,6	68975,47	1,00
NR94ver	Northridge, 1994	LA - E Vernon Ave.		5,61	20,11	14,50	17092,03	30,0	17092,03	1,00
SF71pel	San Fernando, 1971	LA - Hollywood Stor Lot		1,59	19,92	18,33	26690,793	28,0	26933,7152	0,99
SH87bra	Superstition Hills, 1987	Brawley		4,00	19,97	15,97	13407,527	22,1	13619,4572	0,98
SH87icc	Superstition Hills, 1987	El Centro Imp Co. Cent		4,70	39,75	35,05	66165,433	40,0	66166,1256	1,00
SH87pls	Superstition Hills, 1987	Plaster City		4,08	20,33	16,25	38716,632	22,2	39125,2054	0,99
SH87wsm	Superstition Hills, 1987	Westmorland Fire Station		4,01	31,05	27,04	49242,672	40,0	49910,2089	0,99
			Average =	4,32	23,69	19,37	4,15E+04		4,26E+04	96,74%
			σ =	1,33	6,97	6,58	3,68E+04		3,76E+04	3,54%

t_1:	Time at which the Power of the record begins to increase from zero	T:	Record length (sec)
t_2:	Time at which 94% (on average) of the Power is reached	P_e	Power at the end of the record
$t_2 - t_1$:	Rise time necesary to increase the Power from zero to 94% (on average)		
P_{t2}	Power at t_2 reaching 94% (on average) of the maximum Power (Pe)		

The first important difference, observing the FDR, the BDR and the ordinary records data (table 2) is the time rise of the Power. Taking out the Landers BDR and FDR, which show unexpected rise times, the average rise time for the BDR is 10.82 sec, for the FDR is 6.82 sec and for the ordinary records is 17.9 sec. That is, since the BDR have a more distributed acceleration amplitude along the time, the rise time increases to 1.6 times that of the FDR and since the ordinary records have an even wider distribution of the amplitudes the rise time increases 2.6 times that of the FDR.

Another important difference in regard to the 3 types of records: BDR, FDR and ordinary, is in the level of the Power, Pt_2, reached at the end of the rise time, t_2. On average, this Power, for the FDR, is 1.3 times that of the BDR and 6.8 times that of the ordinary records. The relation Pt_2/Pe is, on average, 94% for the NFGMR and 96.7% for the ordinary records. The standard deviations are 3.76% for the BDR, 3.52% for the FDR and 3.5% for the ordinary.

It is important to emphasize that the NFGMR reach a quite larger Power than the ordinary records during a very small rise time.

Fig 4 shows the Power of the records which Fourier spectra are shown in Figure 3. It results interesting to compare the Power the NR94stc record of the 1994 Northridge earthquake, which is an ordinary record, with the Power of the EZ92erzi record of the 1992 Erzincan earthquake which is a Near Fault record. The rise time of the Power at t_2 is 20.18 sec for the former and 2.95 sec for the latest.

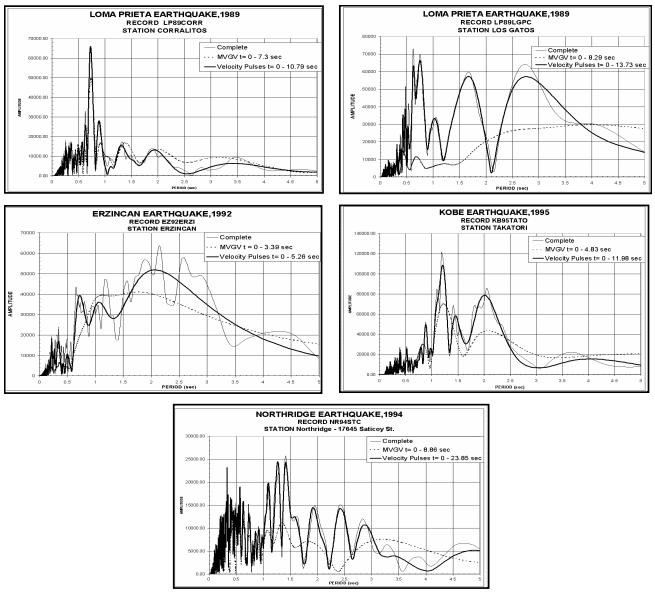

FIGURE 3. FOURIER SPECTRA

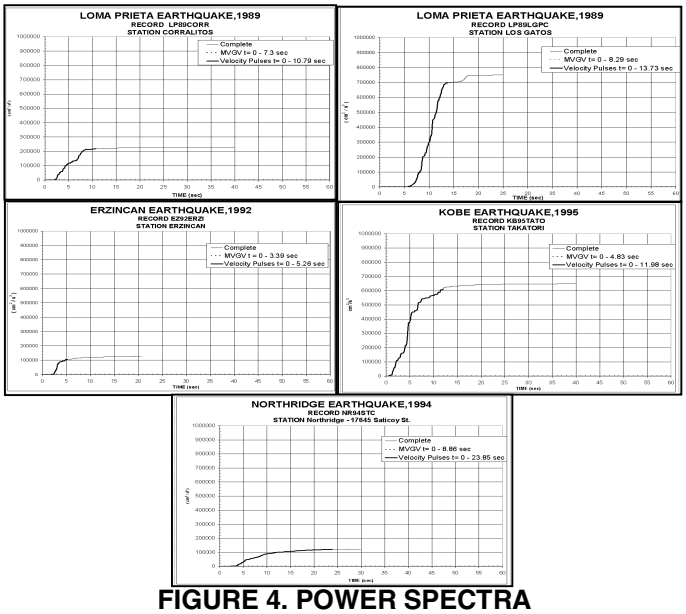

FIGURE 4. POWER SPECTRA

From tables 1 and 2 it is evident that:

1. NFGMR concentrate most of their energy in a very short interval of time, 6.8 sec for the FDR and 10.82 sec for the BDR, during the first 11 seconds, on average, of the ground motion.
2. For FDR and BDR, the Power reached at the end of this short interval of time is, on average, 94% of the total Power reached at the end of the record.
3. On ordinary records, the Energy is more distributed along the time. On average, 96.7% of the total Power is reached in an interval of time of 17.9 sec during the first 22 sec of the ground motions.
4. Completion of the 94% of the Power for FDR and BDR as well as completion of the 96.7% of the Power for ordinary records allows to include all important velocity pulses contained in the ground velocity and most of the frequency or period content of the record. The corresponding duration will be called the effective duration of the record.
5. Determination of the MVGV allows to identify the presence of severe pulses, from the point of view of the record, in any ground motion obtained near or far from the fault. The severity of a pulse on SDOF structures will be studied later through the inelastic response.
6. The cuts above indicated clearly demonstrate that the response depends not only on the MVGV, but on the motion before and after the MVGV.

Elastic Strength Demand Spectra (ESDS). ESDS have been developed for the complete record, the first cut and the second cut. Figure 5 shows the ESDS for the records already discussed through figures 3 and 4.

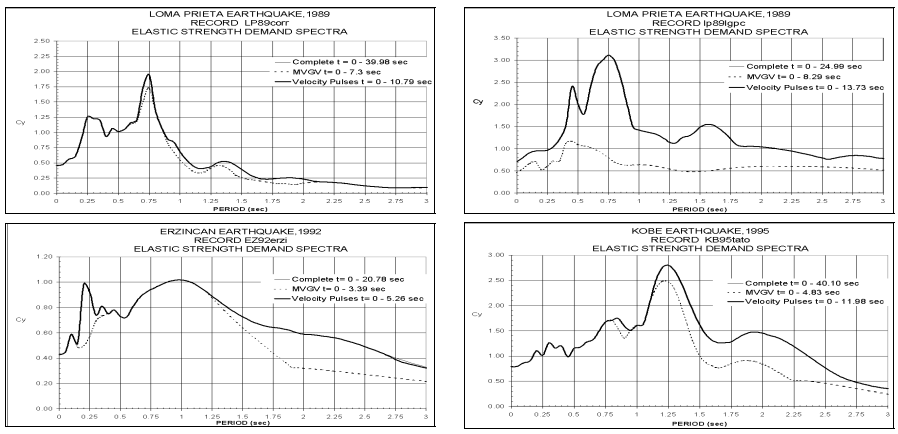

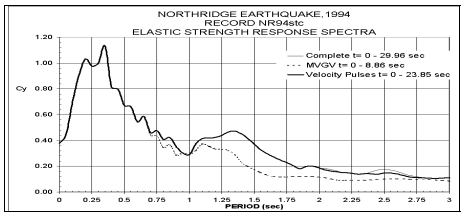

FIGURE 5. ELASTIC STRENGTH DEMAND SPECTRA

Since the first cut does not contain much of the period content of the complete record, the correspondent ESDS are very different from those of the complete record. The piece of record corresponding to the second cut or effective duration of the record, shows an almost perfect match with the EDS of the complete record and is indicating that the period content of the motion before and after the MVGV is very important.

Comparison of ESDS of FDR and BDR with respect to ESDS of ordinary records. Figure 6 shows the 84 percentile spectra of the ESDS of the 15 FDR, the 7 BDR and the 40 ordinary records. Since, in general, the maximum acceleration of the NFGMR is larger than that of the ordinary records (Table 1) the spectral acceleration of the NFGMR shows the same tendency.

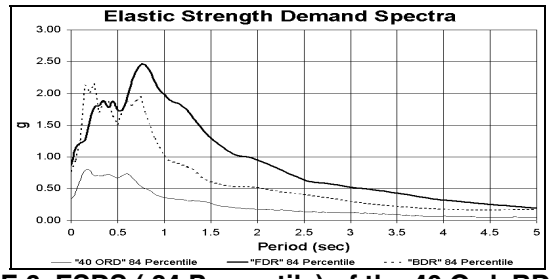

FIGURE 6. ESDS (84 Percentile) of the 40 Ord, BDR, FDR

The main difference, in regard to the period content of the records can be observed in figure 6. While the maximum spectral amplitudes of the FDR and BDR do not show a large difference and occur at about the same range of periods, the difference between those and the ordinary records is important. The amplitudes are extremely different and occur at slightly different periods. The period at which the decay of the ordinates begins is about 0.75 sec for the FDR and BDR and 0.6 for the ordinary records.

The decay curves for the FDR and BDR are more pronounced than those of the ordinary records and the difference in ordinates of the three 84 percentile spectra are very large in the medium range of periods. For example for T = 1.5 sec, the spectral accelerations are: 1.3 g for the FDR, 0.6 g for the BDR and 0.25 g for the ordinary. The tendency decreases for long periods.

It should be mentioned that from the point of view of designing elastically for a NFGMR, the 84 percentile of the FDR with the parameters that will be described immediately after, should be considered since it is not possible to determine, beforehand, if the structure is going to receive the propagation wave (forward directivity effect) or if it is going to be behind such propagation (backward directivity effect).

Comparison of ESDS of the FDR vs. UBC-97 [6]. Figure 7 shows the ESDS for the 15 records showing forward directivity effects (FDR). In the same figure the average spectra of the 15 records and the 84 percentile spectra as well as the UBC-97 [6] spectra are shown.

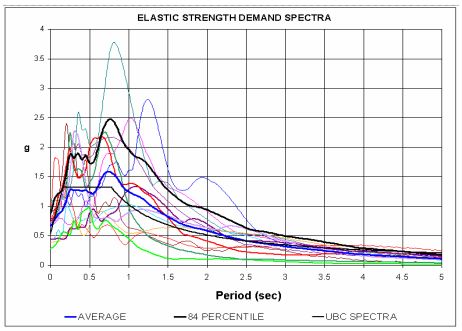

FIGURE 7. ESDS (84 PERCENTILE) OF THE NFGR, UBC

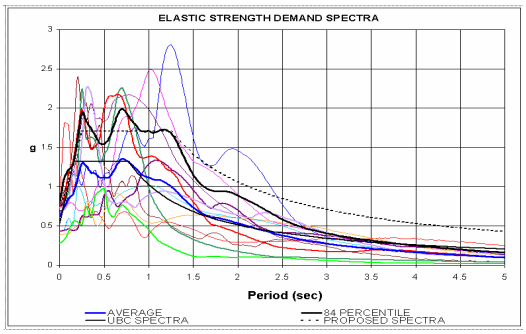

FIGURE 8. ESDS (84 PERCENTILE) OF THE NFGR WITHOUT KB95kobj & LP89lgpc

As it can be observed in Fig 7, the average spectra coincides with the UBC-97 [6] spectra but both are very different from the 84 percentile spectra. This has a large peak at about T=0.75 sec which is due to the peaks shown by the ESDS corresponding to the KB95kobj and the LP89lgpc records. If these records are taken out, the 84 percentile spectra of the 13 FDR left is shown in figure 8. The smooth spectra that represents the 84 percentile spectra is shown in the same figure. Figure 8 also shows the UBC-97 [7] spectra recommended for soil profile S_d, seismic source type A and distance from the site to the fault equal to 2 Km. It results evident that the recommended UBC-97 [6] spectra contains very low ordinates compared to the 84 percentile of the 13 FDR, and the corners of the UBC-97 [6] spectra, defined by T_0 and T_s, differ significantly from the 84 percentile spectra of the 13 FDR. For these reasons the smooth spectra representing the 84 percentile spectra (Fig 8) is recommended in this investigation to be used for elastic analysis of structures located near the Fault. The parameters for this recommend spectra are:

$$C_a = 0.44,\ T_0 = 0.25,\ T_s = 1.25,\ C_v = 0.64,\ \ N_a = 1.55,\ N_v = 3.33$$

INELASTIC PROCEDURES TO UNDERSTAND THE INELASTIC RESPONSE OF SDOF STRUCTURES SUBJECTED TO EQGMR's CONTAINING SEVERE PULSES.

Inelastic Demand Spectra (IDS). Figure 9 shows the Inelastic Strength Demand Spectra (ISDS) for constant cyclic ductility ratio, $\mu_c = 6$, obtained for some of the FDR, BDR and ordinary records shown in table 1. Clearly, the effective duration of the record, obtained through the Power, matches with the ISDS of the complete record indicating again that the period content of the motion before and after the MVGV is very important and most be considered for elastic and inelastic demand spectra and that if all the important velocity pulses after the MVGV are not considered, the recreation of the ISDS is not possible. The model used for the ISDS is elastic-perfectly plastic (Fig 10).

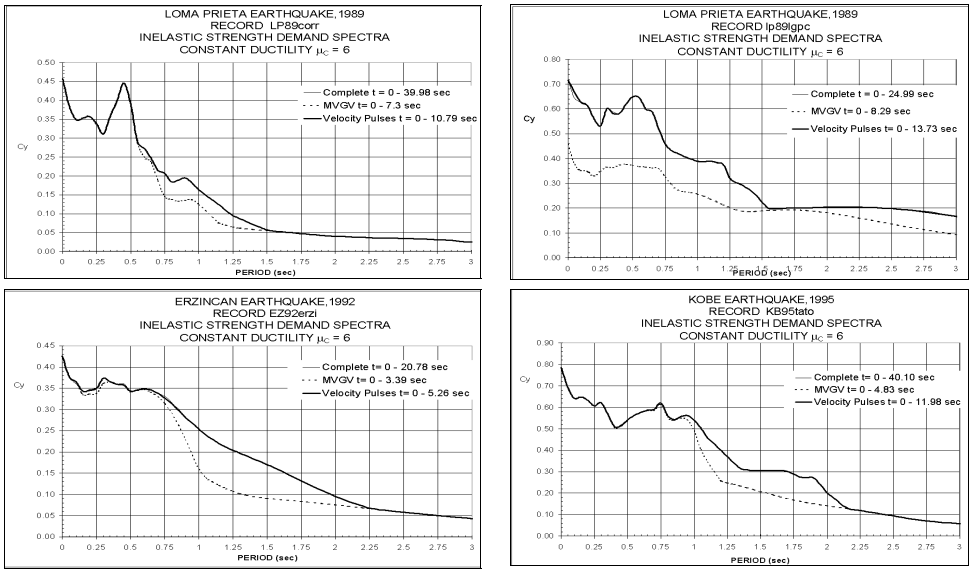

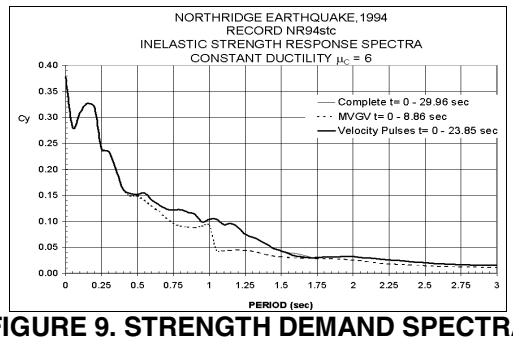

FIGURE 9. STRENGTH DEMAND SPECTRA FOR CONSTANT CYCLIC DUCTILITY

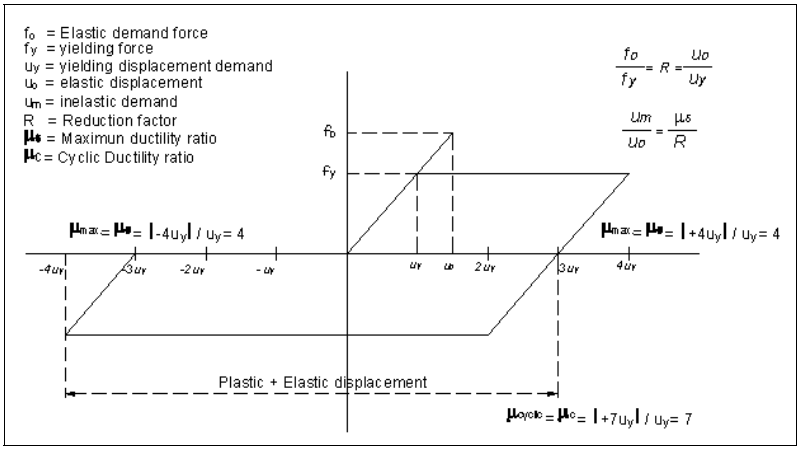

FIGURE 10. ELASTIC-PERFECTLY PLASTIC RESISTANCE FUNCTION

It is important to notice that the proposed procedure of obtaining the Power, before described, allows to obtain a good representation of the period content as well as a reliable elastic and inelastic demand spectra.

An important feature of the IDS presented in figure 9, is the use of cyclic constant ductility ratio, μ_c, defined as

$$|\mu_c| = |u_c| / u_y \qquad (1)$$

$|u_c|$ is the maximum plastic cumulative displacement demand plus the yielding displacement. It is the envelope of the force-displacement relationship. (Fig 10).

$|\mu_c|$ is the cyclic ductility ratio which is different from the so called maximum ductility ratio. In the latest the maximum displacement is measured from the previous displacement zero crossing whereas the cyclic ductility takes into consideration the fact that there might be yielding in the two directions of motion.

The numerical difference can be observed in the example shown in figure 10 where the maximum ductility ratio is equal to 4, since the absolute value of the displacement, measured from zero displacement, at both sides of the abscissa is 4, and the yield displacement is equal to one. However, the cyclic ductility is equal to 7, since the cyclic displacement takes into consideration the yielding in both directions of motion, measured from the zero force crossing of the envelope, which is equal to seven, and the yield displacement is still equal to 1.

The advantages of defining the IDS with respect to the cyclic ductility ratio instead of the maximum ductility ratio are:

1. To avoid sudden jumps in the IDS for constant ductility. These jumps are produced when the SDOF structure crosses from positive to negative displacement or vice versa. When the cyclic displacement is not considered, the maximum constant ductility ratio results from dividing the maximum displacement, measured from the previous zero displacement crossing, with respect to the yield displacement. As can be seen in figure 10 this maximum displacement is shorter than the cyclic displacement. Therefore, in order to keep the constant value of the maximum ductility ratio chosen, the spectral curve must jump down to accommodate the smaller displacement.
2. To obtain a better approximation of the real ductility ratio demanded by the ground motion to the SDOF structure. During actual earthquakes, as the structure increases its excursion into the plastic range, the probability of having reversals in the displacements increase, and so the plastic displacement (Fig 10). The plastic displacement means damage and therefore, for analysis, the maximum plastic displacement, including reversals, should be considered.

Maximum ductility ratio vs. cyclic ductility ratio. Even though, the ISDS, for constant cyclic ductility ratio, is a more reliable measure of the inelastic response of SDOF structures it should be recognized that the information given by the ISDS must be completed with the total displacement (u_m) that includes the plastic and the yield displacements of the SDOF. This total displacement for each period is presented herein in the form of a Physical ductility spectra (PDS) where the reversals of plastic displacement have been taking into account, for μ_c = 2, 4, 6, 8 (Fig 11).

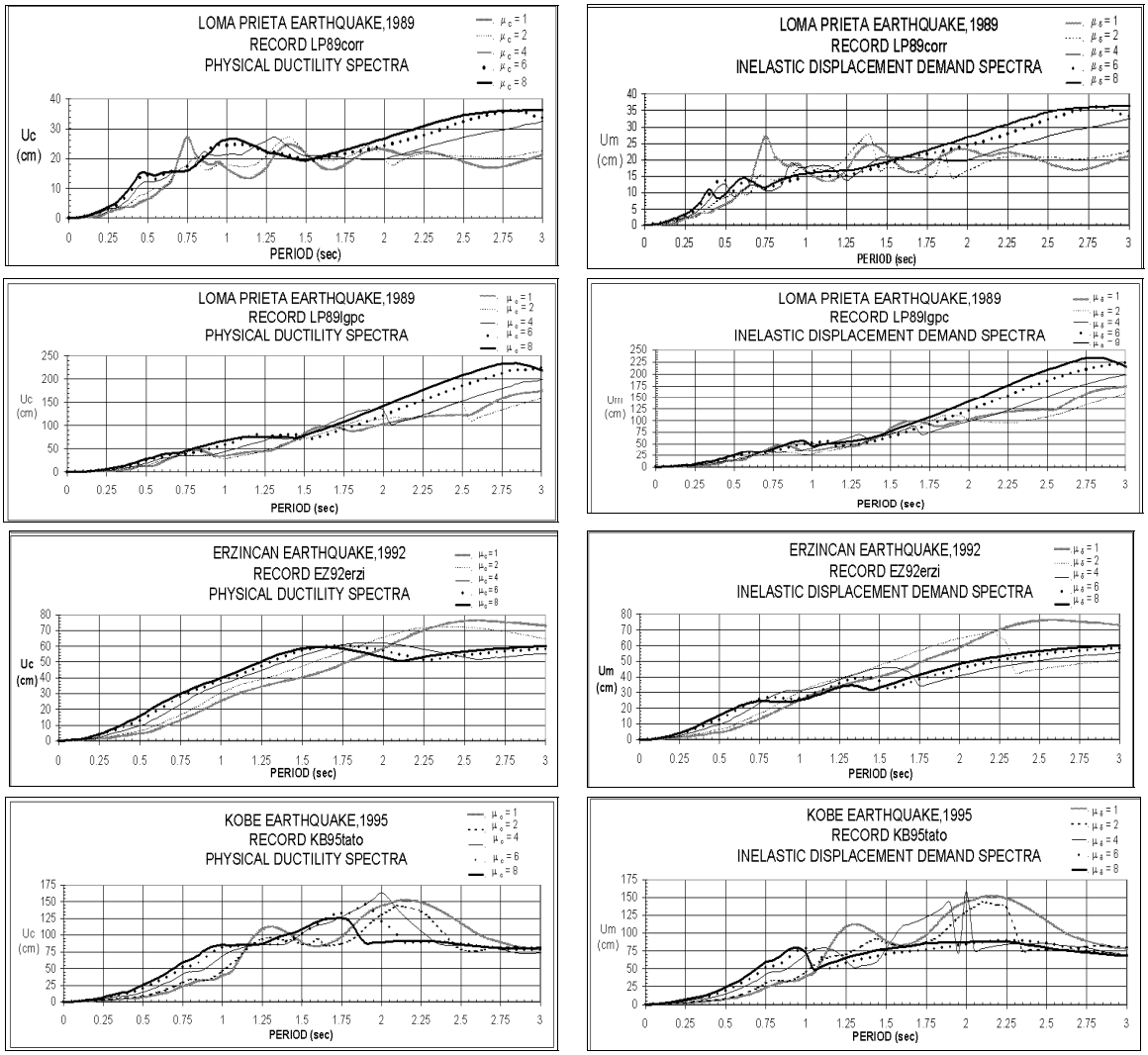

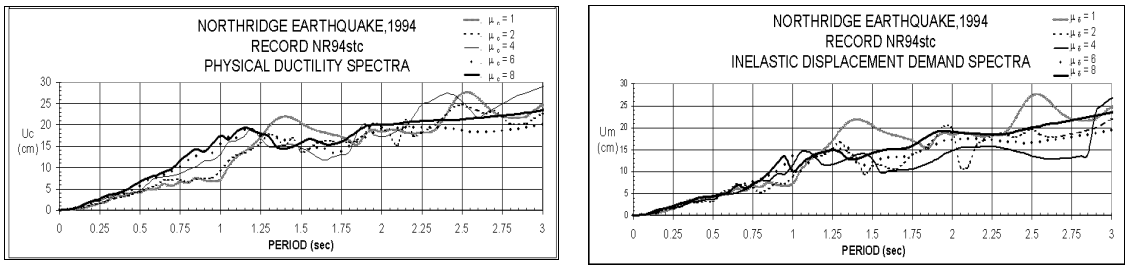

FIGURE 11. CYCLIC DUCTILITY RATIO VS. MAXIMUM DUCTILITY RATIO

On the other hand, the same figure shows the inelastic displacement demand spectra (IDDS) for maximum ductility ratio ($\mu_\delta = 2, 4, 6, 8$). Comparison of the displacements demanded by some of the ground motions listed in table 1 using cycle ductility ratio or maximum ductility ratio is summarized as follows:

	LP89corr		MH84cyld		KB95kobj		KB95tato		IV79ar06	
μ_c	T_1 sec	T_2 sec	T_1 sec	T_2 sec	T_1 sec	T_2 sec	T_1 sec	T_2 sec	T_1 sec	T_2 sec
2	1.4	2.1	0.45	2.7	0.6	2.2	1.1	1.3	4	
4	0.6	1.4	0.4	2.8	0.6	2.8	1.1	2.5	3	4.5
6	0.75	1.75	0.6	2.6	0.7	3	1.1	2.1	2.4	4
8	0.4	1.6	0.25	2.2	0.85	3	0.9	1.9	1.6	3.6

	EZ92erzi		NR94stc		LP89g03		LP89cap	
μ_c	T_1 sec	T_2 sec	T_1 sec	T_2 sec	T_1 sec	T_2 sec	T_1 sec	T_2 sec
2	2.1		0.8		2		1.1	1.8
4	0.8	2.6	0.6		1.4		0.8	
6	0.7	2.2	0.4	2.7	1.1		0.8	
8	0.6	2.1	0.3	2.7	0.9		1.3	

T_1: Period at which the cyclic displacements begins to be larger than the maximum. Before T_1, both are similar

T_2: Period at which the cyclic displacements become equal to the maximum

From the above summary the evidence shows:

1. The sudden jumps that appear in the IDDS induce large decreases in the displacement demand measured according to the maximum ductility ratio.
2. In most of the cases, the displacement demand measured according to the cyclic ductility ratio is a smooth curve.
3. Therefore the main differences in the displacements are due to the fact that while the maximum ductility ratio curve jumps down, the cyclic ductility ratio curve shows no sudden variations.
4. For the KB95kobj, KB95tato and LP89g03 records, the cyclic ductility ratio curves show some jumps. These are due to the fact that these records induce several cycles of force-deformation and since the computation of the cyclic ductility ratio is performed using the maximum plastic displacement, plus the elastic, there is no summation of the several cycles of plastic displacement that overlap one another. Again the total displacement is larger than the maximum plastic plus the elastic, but since the ductility ratio is fixed, the displacement has to go down in order to accommodate for the fixed cyclic ductility ratio.
5. The LP89lgpc record shows the same displacement demand for both: the maximum and the cyclic ductility ratios. This is because the train of pulses of this record push the SDOF in one direction, therefore both displacements are similar.
6. The IV79ar06 record shows similar displacement demands for both ductility ratios up to the period where the sudden jumps occur in the maximum ductility ratio curves. For the EZ92erzi record occurs a similar situation but only for $\mu_\delta = 2$.
7. The NR94stc, the LP89g03 and the LP89cap ordinary records show a similar trend as above for more ductility ratios.

Inelastic time-history responses. The proposed procedure of using the Power of the ground motion, so far has demonstrated that it is possible to obtain reliable elastic and inelastic demand spectra. However, it is necessary to study the nonlinear time-history response of structures subjected to the effective length of the record in order to determine what is a severe pulse from the point of view of the structure and which are the periods of the structures that result more affected by ground records obtained near or far from the fault.

In what follows a linear elastic-perfectly plastic model is used for calculating the response of SDOF structures subjected to the 10 FDR, BDR and ordinary records that have been studied before. Four different values of constant cyclic ductility ratio (μ_c= 2, 4, 6, 8), which was defined above, (Fig 10), were used to limit the response and to observe how the effective length of the record affects the inelastic response of structures.

Figure 12 shows some of the inelastic time-history responses (ITHR's) for μ_c = 6, of SDOF structures subjected to the ground motions listed in table 1. The first inelastic excursion, the maximum positive and negative plastic displacement, the time at which the above occurs and what causes each one of the above events can be seen in the following summary that covers 10 of the ground motions listed in table 1.

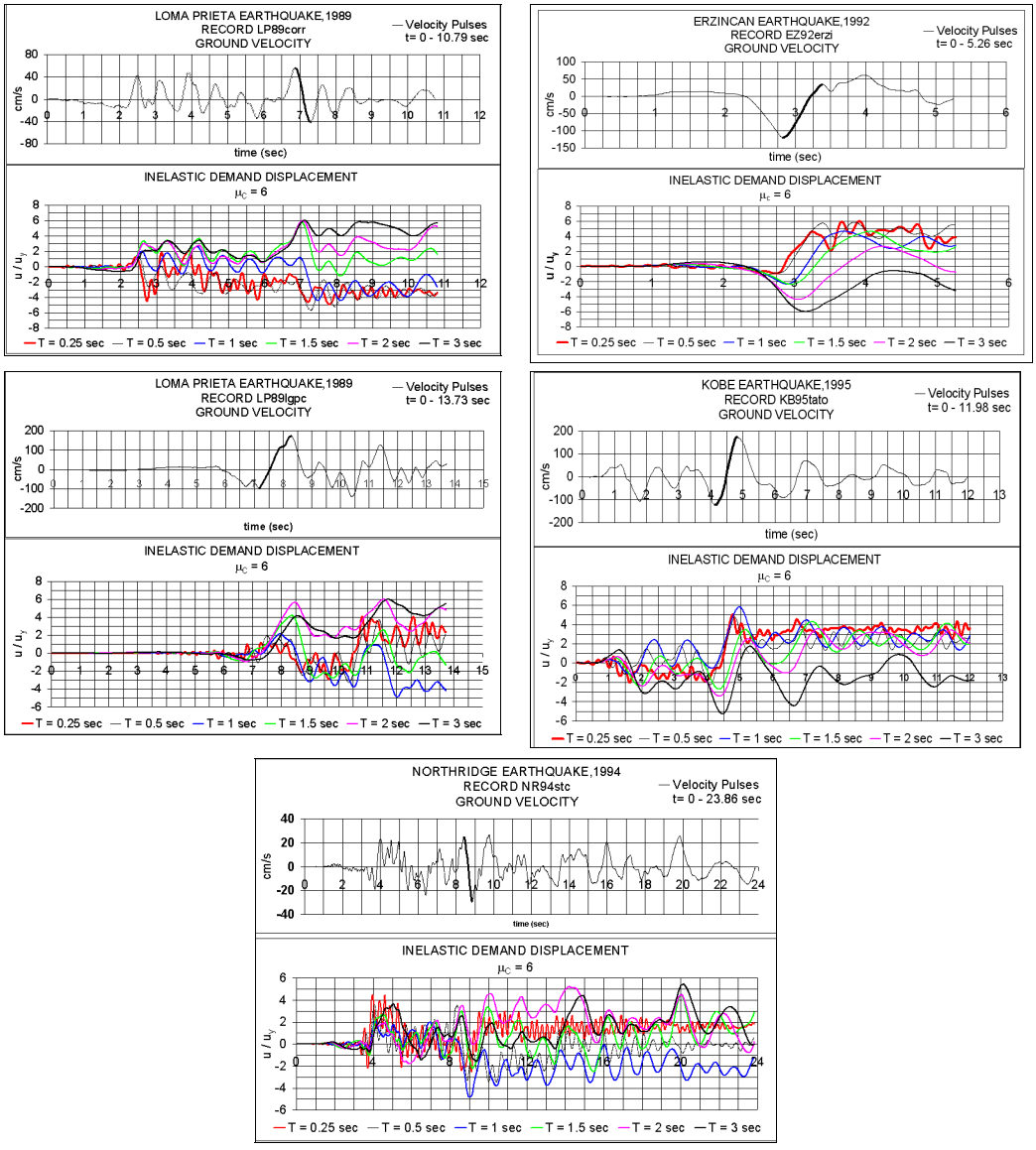

FIGURE 12. INELASTIC TIME-HISTORY RESPONSES

Record	T (sec)	First excursion (at t=sec)	MPPD (at t = sec)	MNPD (at t=sec)
LP89corr	0.25	VGV (2.4)	VGV (3.9)	VGV (7.6)
(BDR)	0.5	VGV (2.5)	VGV (3.9)	MVGV (7.3)*
	1.0	VGV (2.5)	VGV (4.2)	MVGV (7.4)*
	1.5	VGV (2.6)	VGV (7.0)	VGV (8.1)
	2.0	VGV (2.6)	VGV (7.0)	
	3.0	VGV (2.6)	VGV (7.0)	
MH84cyld	0.25	VGV (3.6)	VGV (3.6)	VGV (4.2)
(FDR)	0.5	VGV (3.3)	VGV (3.3)	VGV (3.4)
	1.0	VGV (3.3)	VGV (3.4)	VGV (5.3)
	1.5	VGV (3.3)	VGV (3.4)	VGV (5.4)
	2.0	VGV (3.3)	VGV (3.4)	VGV (5.4)
	3.0	VGV (2.7)	VGV (3.5)	
KB95kobj	0.25	VGV (7.5)	MVGV (8.1)	
(FDR)	0.5	VGV (7.6)	MVGV (8.1)	
	1.0	VGV (7.7)	VGV (10.6)	VGV (7.4)
	1.5	VGV (7.7)	MVGV (9.0)*	VGV (7.4)
	2.0	VGV (7.8)	MVGV (9.2)*	VGV (7.5)
	3.0	VGV (7.2)	MVGV (9.4)*	VGV (8.4)
LG89lgpc	0.25	VGV (8.6)	VGV (10.3)	VGV (9.6)
(FDR)	0.5	MVGV (7.4)	VGV (11.4)	VGV (10.4)
	1.0	MVGV (7.6)	MVGV (7.9)	VGV (12.0)*
	1.5	MVGV (7.6)	MVGV (8.3)*	VGV (9.1)
	2.0	MVGV (7.6)	VGV (11.5)	
	3.0	MVGV (7.7)	VGV (11.6)	
KB95tato	0.25	VGV (1.3)	MVGV (4.7)*	VGV (1.6)
(FDR)	0.5	VGV (1.4)	MVGV (7.6)*	VGV (4.1)
	1.0	VGV (1.5)	MVGV (4.9)*	VGV (1.6)
	1.5	VGV (1.6)	VGV (7.3)	VGV (4.3)
	2.0	VGV (1.7)	VGV (7.4)	VGV (4.3)
	3.0	VGV (1.2)	MVGV (5.3)	VGV (4.4)*
IV79ar06	0.25	VGV (4.8)	VGV (5.6)	
(FDR)	0.5	VGV (4.9)	VGV (5.5)	VGV (6.7)
	1.0	VGV (5.1)	VGV (5.2)	MVGV (6.5)*
	1.5	VGV (5.1)		VGV (7.2)
	2.0	VGV (5.1)		VGV (7.3)
	3.0	VGV (5.1)	VGV (5.8)	VGV (7.6)
ER92erzi	0.25	MVGV (2.8)	VGV (3.7)	
(FDR)	0.5	MVGV (3.0)	MVGV (3.3)	
	1.0	VGV (2.6)	MVGV (3.7)*	VGV (2.6)
	1.5	VGV (2.6)	MVGV (4.1)*	VGV (2.7)
	2.0	VGV (2.5)	MVGV (4.3)	VGV (3.1)*
	3.0	VGV (2.5)		VGV (3.3)
NR94stc	0.25	VGV (3.6)	VGV (4.0)	VGV (9.1)
(ordinary)	0.5	VGV (4.0)	VGV (8.2)*	MVGV (8.9)
	1.0	VGV (4.0)	VGV (4.1)	MVGV (9.0)*
	1.5	VGV (4.0)	VGV (9.9)	VGV (15.3)
	2.0	VGV (4.0)	VGV (5.8)	VGV (14.1)
	3.0	VGV (4.0)	VGV (20.1)	VGV (9.3)
LP89g03	0.25	VGV (4.1)	VGV (4.2)	VGV (5.2)
(ordinary)	0.5	VGV (4.1)	VGV (4.4)	MVGV (5.2)*
	1.0	VGV (4.3)	VGV (4.4)	MVGV (5.3)*
	1.5	VGV (4.3)	VGV (4.6)*	MVGV (5.4)
	2.0	VGV (4.3)	VGV (4.6)*	MVGV (5.7)
	3.0	VGV (3.8)	VGV (4.6)*	MVGV (5.9)
LP89cap	0.25	VGV (6.0)	MVGV (9.2)*	VGV (8.1)
(ordinary)	0.5	VGV (6.5)	MVGV (9.2)*	VGV (6.4)
	1.0	VGV (6.5)	VGV (8.7)	VGV (17.2)
	1.5	VGV (5.6)	VGV (8.7)	VGV (6.4)
	2.0	VGV (5.6)	VGV (8.7)	VGV (16.2)
	3.0	VGV (3.4)	VGV (4.0)	VGV (10.4)

MVGV: Maximum variation of ground velocity
VGV: Variation of ground velocity
* Largest inelastic displacement

From the above summary it is clear that:

1. Of the 10 records above indicated, that includes 7 NFGMR's and 3 ordinary records, only the MVGV (270 cm/sec) of the LP89lpgc record and the MVGV (150 cm/sec) of the ER92erzi record induce the first inelastic excursion of the SDOF. The former for 0.5 to 3.0 period structures and the latest for 0.25 and 0.5 period structures.
2. The MVGV of the NFGMR's or of the ordinary records, causes MPPD or MNPD but not for all structures.
3. The MVGV of the MH84cyld (130 cm/sec), which is a FDR, does not cause inelasticity
4. The MVGV of the KB95kobj record induces inelasticity in all period structures studied, except for T = 1.0 sec.
5. In most of the cases the severe pulse represented by the MVGV induces the largest plastic displacement.
6. The severe pulse, for NFGMR's or ordinary records, is not necessarily the one that causes inelasticity. In most of the cases other pulses, represented by variations of ground velocity (VGV), lower than the MVGV, induce inelasticity and some times the largest plastic displacement.
7. Clearly, SDOF structures with T = 0.5 and T = 1.0 are the ones that more times respond inelastically due to the MVGV of the EQGMR's studied.
8. In most of the cases, short period structures (T = 0.25 sec) as well as long period structures (T = 2 and 3 sec) are not affected by the MVGV.
9. In most of the cases, after the largest plastic displacement, the response tends to be one sided.
10. In most of the cases there is more than one complete cycle in the response (Fig 12).

Inelastic Strength Demand Spectra (ISDS). Fig 13 shows the ISDS for cyclic ductility ratio of some of the records listed in table 1. The ordinates are presented in the form of the yielding coefficient, C_y. In this figure only one ISDS, KB95tato record, calculated using μ_δ, is shown for comparison. Clearly the ordinates of the ISDS calculated using μ_c are larger than those calculated using μ_δ. This situation is similar for all ISDS of the other records studied.

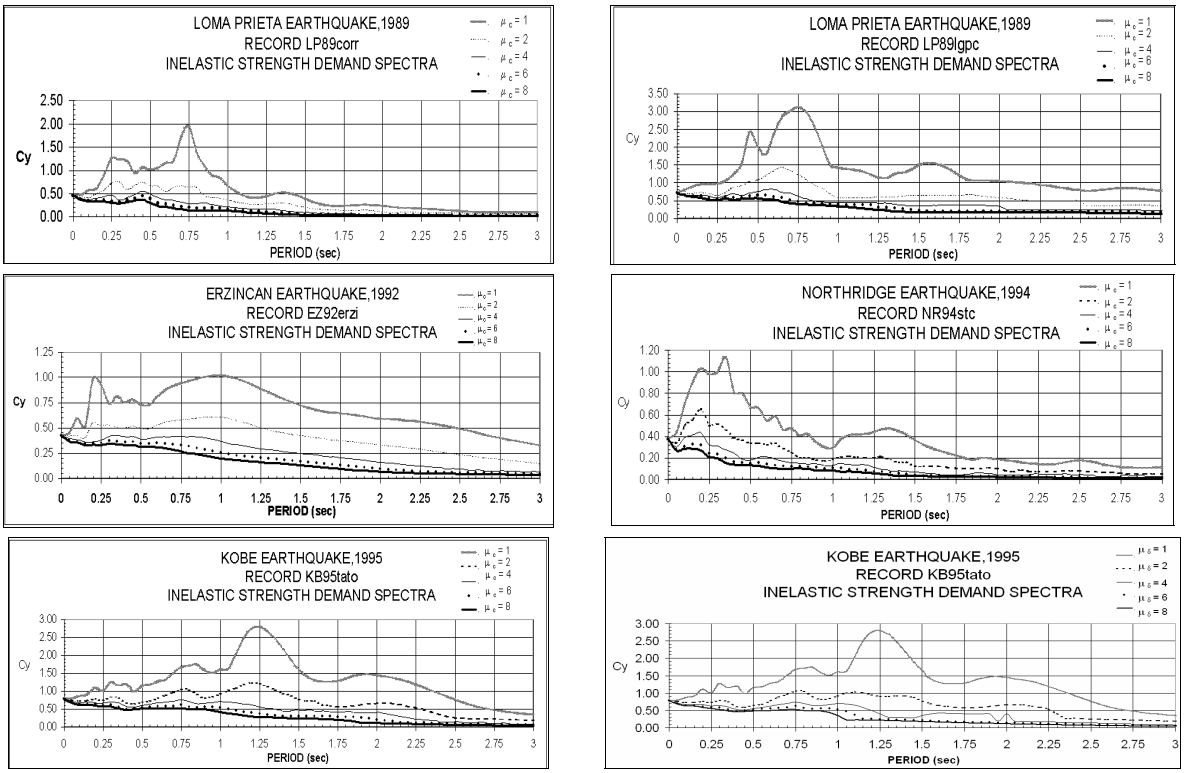

FIGURE 13. INELASTIC STRENGTH DEMAND SPECTRA (ISDS)

CONCLUSIONS

1. The Power of the record is a way to determine what are the variations of ground velocity (VGV) that must be taken into account to obtain reliable Elastic and Inelastic demand spectra.
2. That Power, in the case of NFGMR's, is obtained in very short periods of time. In the case of ordinary records that Power is reached in a longer time.
3. The Power demonstrated that it is not only the MVGV the cause of inelasticity. The VGV before or after the MVGV of any record, near or far from the fault, must be considered in order to obtain reliable demands for design.
4. Every record, near or far from the fault, has its severe pulse that will induce inelasticity for some structures.
5. The cyclic ductility ratio is a measure of the damage the structure suffers during the earthquake. It is calculated according to the global plastic displacement, considering the reversals induced by the ground motions. Therefore is a more reliable measure than the maximum ductility ratio.
6. For some range of periods, particularly when the displacement calculated through μ_δ jumps down, the PDS indicates a larger displacement demand than that of the IDS.
7. The MVGV is not the only cause of inelasticity. Less severe pulses before or after the MVGV cause inelasticity and in some cases the maximum inelastic displacement which includes reversals.
8. The MVGV affect mainly to T = 0.5 and 1.0 sec SDOF structures.
9. The response tends to be one sided after the push given by the MVGV.
10. The ISDS calculated using μ_c show a larger demanded C_y than that calculated using μ_δ. This is due to the fact that plastic displacement that considers the reversals is larger than the maximum measured only from the zero displacement crossing. For a fixed value of μ_c, the reduction factor, R, used to determine the yielding force level, diminishes, therefore the strength demanded by the ground motion becomes larger.
11. The displacement demands obtained with the PDS and the strength demands calculated through μ_c are more reliable because by the reasons above indicated.
12. The PDS are a proposal that comes out of this investigation. The PDS along with the ISDS for constant μ_c, appear as more reliable quantities for design.

ACKNOWLEDGEMENTS

Even though Professor Bertero is one of the Authors, the three first authors recognize his permanent and generous advice and his direction to comply with the objectives of the research.

REFERENCES

1. Sasani, M, Bertero VV, Anderson J. "Rehabilitation of Nonductile RC Frame building using encasement plates and Energy – dissipating devices". Pacific Earthquake Engineering Research Center (PEER). Berkeley: University of California, 1999.
2. Sasani M. Ph.D. Dissertation. Berkeley: University of California, 2000
3. Alavi B, Krawinkler H. "Effects of near-fault ground motions on frame structures". The John A. Blume earthquake engineering center. Department of Civil and environmental engineering. Stanford: Stanford University, 2001.
4. Bertero VV, in collaboration with Herrera R and Mahin S. "Establishment of design earthquakes. Evaluation of present methods". International Symposium on earthquake structural engineering. St. Louis, Missouri, 1976.